

Effect of electron blocking layers on the conduction and valence band profiles of InGaN/GaN LEDs

Simon Hammersley^{*1}, Phil Dawson¹, Menno J. Kappers², Fabien C.-P. Massabuau², Martin Frentrup², Rachel A. Oliver², and Colin J. Humphreys²

¹ School of Physics and Astronomy, Photon Science Institute, University of Manchester, M13 9PL, UK


² Department of Materials Science and Metallurgy, University of Cambridge, 27 Charles Babbage Road, Cambridge, CB3 0FS, UK

Received 30 September 2015, revised 15 January 2016, accepted 26 January 2016

Published online 22 February 2016

Keywords LEDs, electron blocking layers, efficiency, photoluminescence

* Corresponding author: e-mail simon.hammersley@manchester.ac.uk, Phone: +44 161 306 4886, Fax: +44 161 275 1031

 This is an open access article under the terms of the Creative Commons Attribution License, which permits use, distribution and reproduction in any medium, provided the original work is properly cited.

In this paper we investigate the effect of including an electron blocking layer between the quantum well active region and the p-type layers of a light emitting diode has on the conduction and valence band profile of a light emitting diode. Two light emitting diode structures with nominally identical quantum well active regions one containing an electron blocking layer and one without were grown for the purposes of this investigation. The conduction and valence band profiles for both structures were then calculated using a commercially available Schrödinger-Poisson calculator, and a modification to the elec-

tric field across the QWs observed. The results of these calculations were then compared to photoluminescence and photoluminescence time decay measurements. The modification in electric field across the quantum wells of the structures resulted in slower radiative recombination in the sample containing an electron blocking layer. The sample containing an electron blocking layer was also found to exhibit a lower internal quantum efficiency, which we attribute to the observed slower radiative recombination lifetime making radiative recombination less competitive.

1 Introduction Light emitting diodes (LEDs) containing InGaN/GaN quantum wells (QWs) are widely used when high efficiency light emission is required in the ultraviolet [1], blue [2] and green [3] regions of the spectrum. In these LED structures, a thin layer of AlGaN:Mg is often placed between the topmost QW of the LED stack and the p-type GaN contact layer, and is referred to as the electron blocking layer (EBL). The inclusion of an EBL has been reported to result in an increase in external quantum efficiency (EQE) in LEDs [4–6], which was attributed to a reduction in electron leakage from the QW active region into the p-type GaN. It has however also been reported that the inclusion of an EBL in an InGaN LED can also lead to a reduction in the EQE, especially at high carrier densities. This is thought to be caused by the EBL acting as a potential barrier for the injection of holes into the QW active region, as well as the creation of a confining potential between the final QW in the stack and the EBL [7–9].

One of the key properties of QWs based on polar group III-Nitrides is the presence of very strong electric fields

across the QWs. These electric fields cause a separation of the electron and hole wavefunctions, resulting in an increase in the radiative recombination lifetime within the sample [10–12]. The inclusion of additional layers with different polarisation constants and doping levels into the structure of the QW will also affect the strength of the total electric field across the QWs in the active region, leading to a further modification to the radiative recombination rates within the LED. It has been suggested that such an effect occurs when an EBL is included within a quantum well stack [13, 14]. In this paper we investigate the effect that the inclusion of an EBL in the structure of an LED has on its conduction and valence band profiles and measured the resultant changes in the radiative recombination rate using low temperature PL decay measurements. Temperature dependent photoluminescence (PL) spectroscopy are then used to see how this modification to the radiative recombination lifetime effects the internal quantum efficiency of the LED.

2 Experimental details Two LED structures were grown using metalorganic chemical vapour deposition on sapphire substrates, on which 2.5 μm of nominally undoped GaN was deposited as a pseudo substrate. Following this 2.7 μm of GaN:Si, with a doping density of $4 \times 10^{18} \text{ cm}^{-3}$ was deposited to act as an n-type contact region for the LED, a prelayer [15] consisting of a 23 nm thick layer of $\text{In}_{0.05}\text{Ga}_{0.95}\text{N}:\text{Si}$ with the same doping density as the n-type contact region was included prior to the QW active region, followed by 3 nm of nominally undoped GaN. The QW active region of the LEDs nominally consisted of 5 periods of 2.5 nm $\text{In}_{0.13}\text{Ga}_{0.87}\text{N}$ separated by 7 nm GaN barriers, grown using the two temperature growth method [16]. After the growth of the QWs the sample structures deviated, with one sample including a 12 nm thick layer of $\text{Al}_{0.17}\text{Ga}_{0.83}\text{N}:\text{Mg}$, with a doping concentration of $3 \times 10^{19} \text{ cm}^{-3}$, whereas in the other sample this layer was omitted. 120 nm of GaN:Mg, with a doping density of $3 \times 10^{19} \text{ cm}^{-3}$, was then deposited on both sample structures in order to act as a p-type contact region.

To characterise the thickness and composition of the QW stacks, X-ray diffraction (XRD) was employed, by performing an ω - 2θ scan along the symmetric (002) reflection. However due to the presence of gross well width fluctuations in our samples, the thickness and composition of the QWs could not be uniquely determined. XRD could only tell us about the period (i.e. the QW + barrier thickness), and average indium composition (i.e. the indium content averaged over a period) of the structure. For the sample containing an EBL, the QW/Barrier repeat period and average indium content were found to be $9.1 \pm 0.1 \text{ nm}$ and $3.4 \pm 0.2\%$ respectively, and in the sample without an EBL the values were found to be $9.2 \pm 0.1 \text{ nm}$ and $3.6 \pm 0.2\%$. The values of the QW/Barrier period thickness and the average indium composition are the same for both samples within the experimental error.

For optical measurements the samples were mounted to the cold finger of a temperature controlled closed cycle helium cryostat, with the samples held at Brewster's angle with respect to the collection optics in order to minimise the effects of Fabry-Pérot interference [17]. For temperature dependent PL measurements the continuous wave excitation from a He/Cd laser with an excitation photon energy of 3.815 eV and incident excitation power density of 5 W cm^{-2} was used. For the time decay measurements the frequency tripled output of a mode locked Ti:Sapphire laser was used with a final photon energy of 4.881 eV and an incident peak power density of $100 \text{ MW cm}^{-2} \text{ pulse}^{-1}$.

3 Results and discussion The conduction and valence band profiles of the two LED structures were calculated using the commercial device simulation package nextnano³ [18] under zero bias conditions in order to better represent the experimental conditions. The potential drop caused by the combination of the depletion field between the p and n-type regions of the LED and the change in polarisation

constants at the QW/barrier interfaces were extracted from the calculated conduction and valence band profiles (Fig. 1). It was found that the inclusion of an EBL into the device structure resulted in a reduction in the strength of the depletion field across the QW stack, from 51 to 34 meV nm^{-1} . Since the depletion field opposes the built in field across each QW, this resulted in an increase in the resultant fields across the QWs on insertion of the EBL. The change in the strength of the depletion field is due to the strong electric field across the AlGaIn layer acting in the same sense as the depletion field across the AlGaIn of the EBL caused by the large change in polarisation constants at the GaN/AlGaIn and AlGaIn/GaN interfaces.

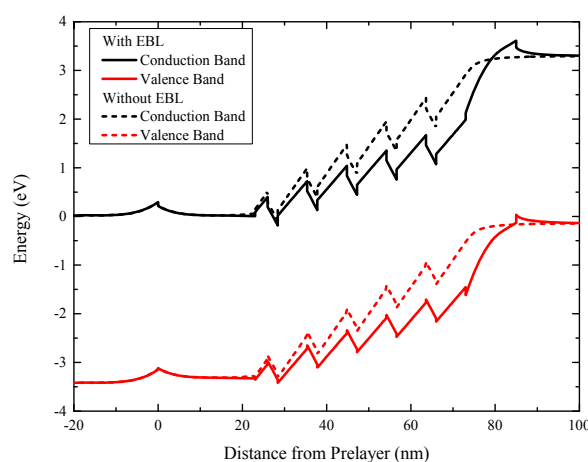


Figure 1 Calculated conduction (black) and valence band (red) profiles for LED structures grown with (solid lines) and without (dashed lines) an EBL under zero bias.

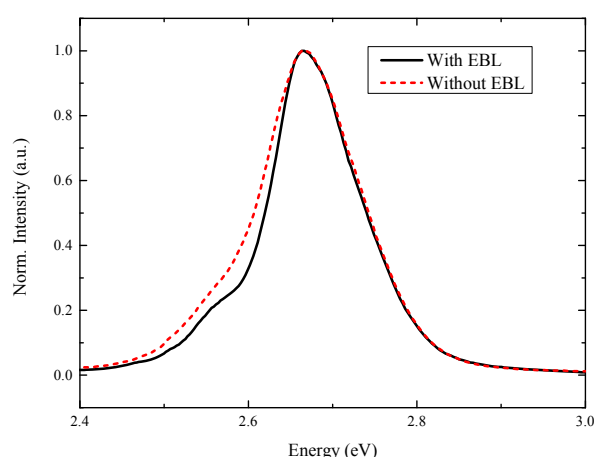


Figure 2 PL emission spectra recorded at 10 K for the sample with (black solid line) and without (red dashed line) an EBL.

The wavefunctions for the electrons and holes within the structure were then calculated from the conduction and

valence band profile, and the energy of the lowest lying electron and hole states in each QW were found. From these wavefunctions the electron/hole wavefunction overlap was calculated for both samples and found to be 20% larger in the sample without an EBL. This change in electron/hole wavefunction overlap suggests that the radiative recombination rate in the sample which does not contain an EBL should be faster than in the structure containing an EBL. The recombination energy for the electron and hole wavefunctions were found to be almost unaffected by the inclusion of the EBL, with the sample with an EBL calculated to have a 4 meV higher recombination energy.

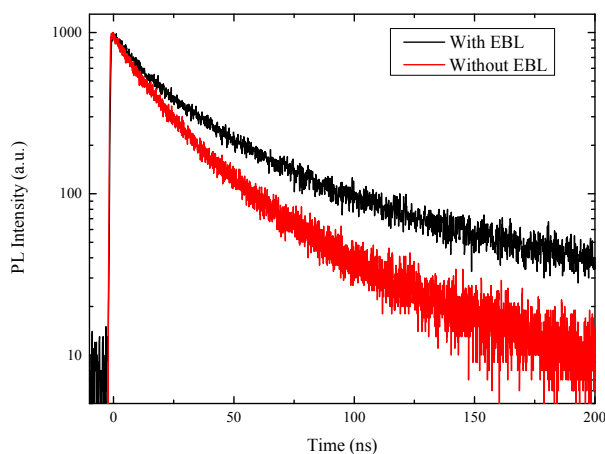


Figure 3 PL decay transients detected at the peak of the PL emission spectrum for the sample with (black line) and without (red line) an EBL.

In order to test these predictions, the optical properties of the two samples were measured. Figure 2 shows the 10 K PL spectra for the two samples, the inclusion of the EBL has not had a measureable effect on the PL peak position. However, there is a slight change in the full width half maximum (FWHM) between the two samples with the sample containing an EBL having a slightly narrower FWHM (121 meV compared with 134 meV for the sample without an EBL). PL decay transients were recorded as a function of detection energy across the luminescence spectra of both samples at 10 K where the PL decay is assumed to be solely radiative [19]. In Fig. 3 are shown the PL decay transient recorded at the luminescence peak for both samples. The transients recorded for the sample including an EBL were found to occur over a longer timescale than that recorded at the same detection energy in the sample where the EBL was not present. As the PL decay transients are non-exponential a single lifetime cannot be extracted, however to allow for quantification of the extent to which the PL decay time has changed the 1/e decay time, defined as the time taken for the PL decay to fall from its maximum value to 1/e of that value, is measured from each decay transient. At the peak of the luminescence spectra the

1/e decay time was found to be 27.0 ± 0.5 and 19.7 ± 0.5 ns for the sample with and without an EBL respectively. In order to improve on the accuracy of this measurement the 1/e PL decay time was measured across the emission, with the sample without an EBL exhibiting a 1/e decay time a $78 \pm 1\%$ of that recorded for the sample with an EBL at all detection energies in line with the calculated change in the electron/hole wavefunction overlap.

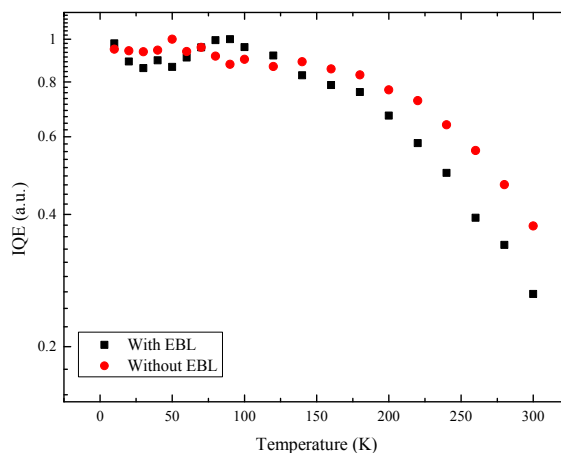


Figure 4 IQE as a function of sample temperature for the sample with (black squares) and without (red circles) an EBL.

The room temperature internal quantum efficiency (IQE) is determined by the competition between the radiative and non-radiative recombination processes. To gauge if the change in radiative recombination rate influences the IQE the PL spectra were recorded as a function of temperature in the range 10–300 K. The IQE at a given temperature was defined using the widely used methodology [20, 21] whereby the recombination at 10 K is assumed to be determined solely by radiative recombination processes and that the ratio between the integrated intensity of the PL spectrum at a given temperature and that recorded at 10 K is the IQE at that temperature. Figure 4 shows the IQE as a function of temperature for both samples, with the sample including an EBL exhibiting a 300 K PL IQE of 26%, and the sample without an EBL exhibiting an IQE of 38%. This finding is in line with the observation of a faster radiative recombination rate in the sample that does not include an EBL.

4 Summary and conclusion In summary, we have investigated the effect that including an EBL has on the conduction and valence band profile of LED structures. Two LED samples with nominally identical QW active regions, one including an EBL and one where the EBL was omitted, were produced and the band profiles calculated, finding that in the sample containing an EBL the resulting potential drop across each QW in the stack was found to be

10% larger than in the sample without an EBL. This change in potential drop across the QW results in a change in the calculated electron-hole wavefunction overlap. Low temperature (10 K) PL decay transients measured on both samples showed that across the PL emission spectrum the PL decay transient in the sample containing an EBL was of the order 20% longer than that for the sample that did not contain an EBL. The 300 K PL IQE was then measured for the two samples, finding that the sample containing an EBL exhibited a lower IQE, 26% compared to 38% for the sample that did not contain the EBL, suggesting that the modification of the PL decay transient has led to less competitive recombination at room temperature in the sample containing an EBL.

This work suggests that in designing LEDs containing EBLs it is necessary to take into account not only carrier overspill but also the impact of the EBL on the conduction and valence band profiles. By careful choice of EBL parameters, such as lower Al contents or higher *p*-type doping levels, or the use of polarisation matched alloys it should be possible to effectively reduce electron leakage without inadvertently degrading the internal quantum efficiency of the QW active region.

Acknowledgements This work was carried out with the financial support of the United Kingdom Engineering and Physical Sciences Research Council under Grant Nos. EP/I012591/1 and EP/H011676/1.

References

- [1] A. Bhattacharyya et al., *Appl. Phys. Lett.* **94**, 181907 (2009).
- [2] Y. Sun et al., *Appl. Phys. Lett.* **87**, 093115 (2005).
- [3] Y. Yang et al., *Appl. Phys. Lett.* **94**, 041117 (2009).
- [4] K. J. Vampola et al., **94**, 061116 (2009).
- [5] A. Knauer et al., *Proc. SPIE* **7231**, 72310G-72310G-9 (2009).
- [6] I. V. Rhozhansky and D. A. Zakheim, *Phys. Status Solidi A* **204**, 227-230 (2007).
- [7] S.-H. Han et al., *Appl. Phys. Lett.* **94**, 231123 (2009).
- [8] J. Piprek, *Phys. Status Solidi A* **207**, 2217-2225 (2010).
- [9] J.-Y. Chang et al., *Opt. Lett.* **35**, 1368-1370 (2010).
- [10] V. Fiorentini et al., *Phys. Rev. B* **60**, 8849 (2008).
- [11] F. Della Sala et al., *Appl. Phys. Lett.* **74**, 2002 (1999).
- [12] F. Bernardini et al., *Appl. Surf. Sci.* **166**, 23-29 (2000).
- [13] Y.Y. Zhang et al., *Appl. Phys. Lett.* **99**, 221103 (2011).
- [14] Y.K. Kuo et al., *Opt. Commun.* **282**, 4252 (2009).
- [15] A. M. Armstrong et al., *J. Appl. Phys.* **117**, 134501 (2015).
- [16] R.A. Oliver et al., *Appl. Phys. Lett.* **103**, 141114 (2013).
- [17] D. Graham et al., *J. Appl. Phys.* **97**, 103508 (2005).
- [15] S. Birner, Nextnano GmbH, www.nextnano.de.
- [19] C. E. Martinez et al., *J. Appl. Phys.* **98**, 053509 (2005).
- [20] A. Hangleiter et al., *Phys. Status Solidi A* **201**, 2808-2813 (2004).
- [21] M. A. Reshchikov et al., *Phys. Status Solidi C* **10**, 507-510 (2013).